[Jaar]

FOM Institute for
Plasma Physics
Rijnhuizen

Nivard Kagie

Utrecht University

Supervisor:

Dr. ir. G.J. De Rooij

CONTINUUM EMISSION AS A DIAGNOSTIC FOR THE ELECTRON DENSITY AT PILOT-PSI

Abstract

Optical emission spectroscopy was used to observe the continuum emission at 700 – 900 nm in a hydrogen plasma at Pilot-PSI in order to extract the electron density out of the absolute intensity of the emission. The validity of the continuum emission diagnostic was judged by comparison with Thomson scattering, which acts as a reliable tool for measuring the electron density. We observed the absolute value of the continuum emission about an order of magnitude higher than the Thomson scattering profile. Moreover, the emission profile over the radius of the plasma beam appears to be hollow, which is not to be expected from the Thomson data. The overcalculation of the continuum intensity is most likely caused by an emission band of molecular hydrogen(715 -765 nm), whereas the hollow emission profile is explained by considering the density of molecular hydrogen, which dominates the emission profile above an electron density of $n_e = 5 \cdot 10^{19}\ m^{-3}$ and hence causes a hollow profile. In conclusion, the 700 – 900 nm regime in a hydrogen plasma is not suitable for extracting the electron density accurately from the continuum emission.

Table of contents

1 Introduction

1.1 Plasma research at FOM Rijnhuizen

As a consequence of the society's growing energy demand, many efforts have been made in order to replace fossil fuels by more sustainable energy sources. For many years nuclear fusion has been mentioned as the ideal solution for the energy problem. In this process, atomic nuclei are *fused* to form a heavier nucleus, accompanied by the release of relatively large amounts of energy, without the production of notable harmful spin-offs.

Unfortunately, constructing a nuclear fusion reactor which is able to produce more energy than was put in, has not yet been realized. However, in France, the International Thermonuclear Experimental Reactor(ITER), is currently being built, which has the goal of investigating the attainability of producing ten times more energy than was put in out of a nuclear fusion reactor. In such a tokamak, the plasma is magnetically confined to a donut-shape in order to achieve nuclear fusion, as shown in fig. 1.

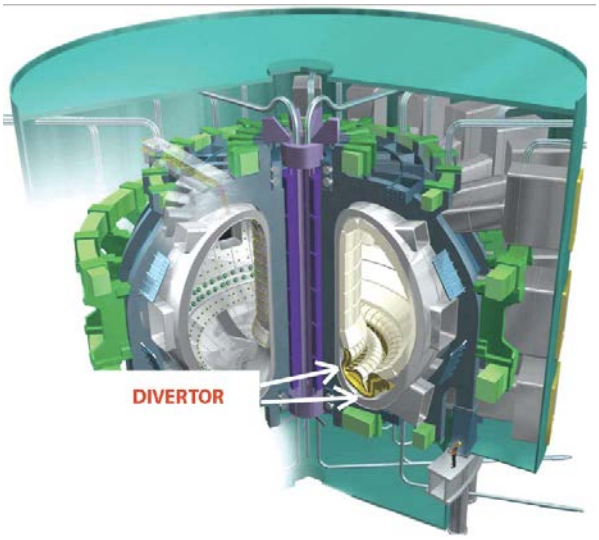

Fig.1 The ITER design with our region of interest: the

The FOM-institute DIFFER in Nieuwegein, The Netherlands, contributes to the ITER-project by investigating plasma-surface interactions of ITER's *divertor*, one of the crucial parts of a tokamak where impurities can be extracted from the plasma. At this place, the plasma strikes the vessel wall, and causes extremely high energy and particle fluxes. DIFFER's linear plasma generator Pilot-PSI, which was used as a forerunner for the currently operating Magnum-PSI, gets close to ITER-relevant conditions in terms of plasma temperature and particle fluxes in order to study plasma-surface interactions.

1.2 Continuum emission as a diagnostic

In plasma physics we'd like to have several reliable diagnostics for measuring the relevant physical properties, such as the electron density(n_e) and temperature (T_e). When investigating plasma-surface interactions, the importance of accurately measuring these quantities cannot be underestimated, as the electron density and temperature determine many crucial processes. For instance, the balance between ionization and recombination, the flux density towards the target(the surface sample that's investigated) and the mean free paths for collisions and ionization are all determined by both n_e and T_e [1].There are several methods for measuring these quantities, such as a Langmuir probe, Thomson scattering and optical emission spectroscopy. In principle, continuum emission, i.e. the 'off-set' of the observed spectrum of the plasma, could be used as a tool for determining the electron density and temperature.

In this thesis we'll examine the spectrum of the hydrogen plasma at Pilot-PSI in order to verify any continuum emission in the plasma light. The part of the spectrum that should theoretically be suitable for continuum measurements is the 700–900 nm range, since there is no contaminating line-radiation in this wavelength regime. Therefore, our focus for the continuum measurements will be on this part of the near infrared spectrum. If this continuum is actually observed in the spectrum, the question arises whether this continuum emission can be used as a good diagnostic. In order to answer this question, we performed Thomson scattering measurements, which serves as a highly proven diagnostic in plasma physics[2], and compared both.

2 Experimental set-up Pilot-PSI

The experiments described in this thesis were performed on the linear plasma generator Pilot-PSI. In this section, an overview of the set-up is provided as well as a detailed description of the diagnostics we used, the plasma producing cascaded arc and its operational details.

2.1 Overview Pilot-PSI

In fig. 2 the Pilot-PSI set-up[3] is schematically shown.

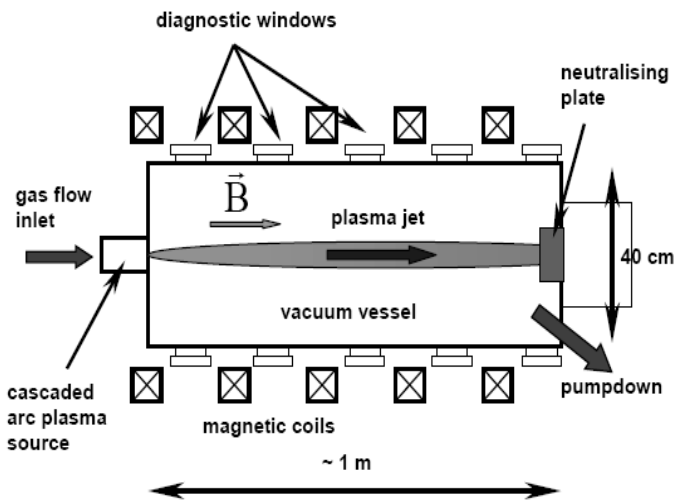

Fig. 2 Pilot-PSI's experimental arrangement

A plasma jet, generated by a cascaded arc plasma source, expands into the 1 m long vacuum vessel due to a high pressure gradient, where it is magnetically confined by oil-cooled coils delivering axial magnetic fields ranging from 0.4 to 1.6 T. In front of the third window of the vessel, the plasma jet impinges on a water-cooled target. Along the side of the vessel, five windows are mounted in order to be able to install diagnostic equipment on the desired axial position.

2.2 Cascaded arc plasma source

In Pilot-PSI a cascaded arc plasma source is mounted, suitable for operation on argon and hydrogen, as shown in Fig. 3.

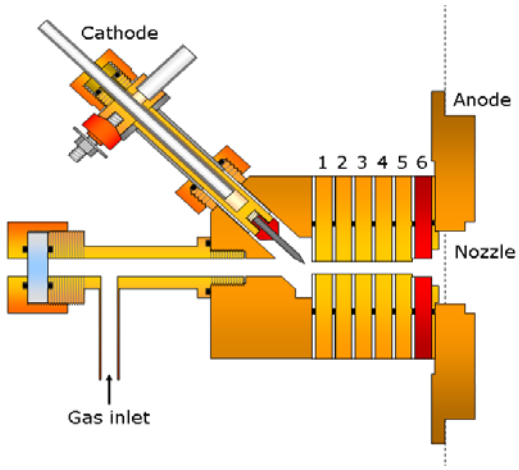

Fig. 3 cross-section of the cascaded arc.

Six electrically insulated copper plates provide a gradual drop in potential between anode(grounded) and cathode(negatively charged), creating a discharge channel that ionizes the gas up to 10% [4] before entering the vessel. The working gas continuously flows into the arc at a pressure of 1-2 x 10^4 Pa, causing the partly ionized gas to supersonically flow into the vacuum vessel(~5 Pa).

2.3 Magnets

As mentioned before, the objective is to establish conditions comparable to those at the divertor in ITER. In order to achieve such high particle fluxes and electron densities and temperatures, the plasma beam needs to be confined on the path towards the target, where the actual plasma-surface interaction takes place. In Pilot-PSI, oil cooled magnets with magnetic field strengths from 0.4 till 1.6 T are responsible for this confinement due to the resulting ExB-drift of the charged particles. At higher fields, only short time 'shots', down to 3 s at 1.6 T, can be taken due to the limited cooling of the magnets. The gyration of the particles around the center of the plasma jet reaches velocities of up to 10^4 m/s and yields a beam diameter of roughly 1 cm[5].

2.4 Plasma diagnostics

In the introduction, the importance of reliable diagnostics for the characterization of the plasma has already been designated. The lay-out of the Pilot-PSI set-up offers several different techniques to measure the relevant plasma parameters accurately. In this thesis, we'll only discuss Thomson scattering and optical emission spectrometry as these techniques were used in our experiments.

2.4.1 Thomson scattering

In Pilot-PSI, determination of the electron density and temperature is mostly done by performing Thomson scattering measurements, which involves scattering by free electrons in the plasma[2]. The electric field of the incident laser light accelerates the electrons, which in turn emit light with the same frequency as the incident light. Since the scattered light is directly proportional to the electron density, the latter can be determined after absolute calibration of the Thomson scattering set-up, which is shown in fig. 4. Besides the density, also the electron temperature can be determined by Thomson scattering. Because of the high velocities of the

electrons in the plasma, the scattered light is Doppler shifted, which yields a Gaussian shaped velocity distribution. The width of this Gaussian is a measure for the electron temperature T_e.

The system is capable of measuring electron density and temperature profiles of a plasma column of 30 mm in diameter with a spatial resolution of 0.6 mm and an observational error of 3% in the electron density n_e and 6% in the electron temperature T_e at $n_e = 4 \times 10^{19}$ m^{-3}[2].

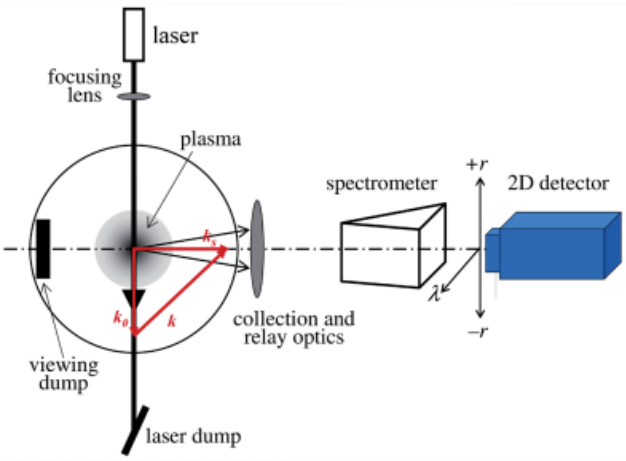

Fig.4 Schematic overview of the Thomson scattering system at Pilot-PSI[2]. Laser light enters the vessel from above and is scattered sidewards by the electrons, where it's detected and analyzed.

2.4.2 Emissivity measurement set-up

Data of our continuum measurements were obtained by using a Phantom CMOS camera, which was installed in front of the first window of the vessel in order to analyze the lateral profile of the emission from the plasma, just in front of the nozzle. A lens of 3500 mm focal length was used to focus the plasma light onto the chip of the camera, after passing a Semrock FF01-filter with a central wavelength of 794 nm and a width of 160 nm, as depicted in Fig. 5.

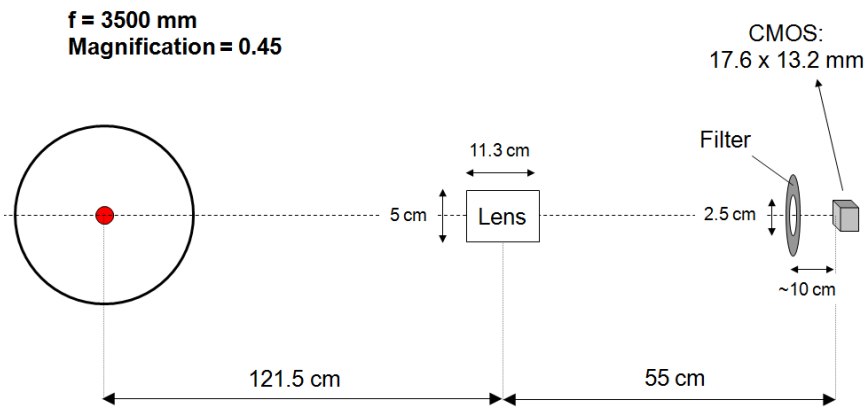

Fig. 5 Schematical overview of the setup , using a high focal length lens, a Semrock-filter and a CMOS camera.

In order to be able to calculate the electron density from the continuum emission, we have to know its absolute intensity. Besides subtracting averaged background from the images, one has to know the sensitivity, and thus the quantum efficiency, of the Phantom camera, since these values enable you to calculate the actual number of photons emitted by the plasma. This quantum efficiency was found using the graph in Fig. 6.

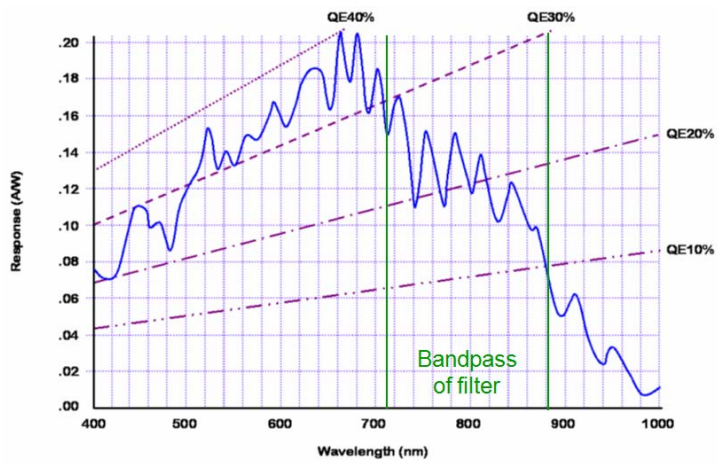

Fig. 6 Spectral response of Phantom CMOS camera.[6]

Furthermore, an absolutely calibrated Labsphere Integrating Sphere was used. This lamp emits a well known spectrum, yielding a wavelength dependent conversion from photon numbers to counts.

3 Theory continuum emission

3.1 Origin of continuum emission

If we're having a close look at plasma radiating processes, we can distinguish two types: continuum and line radiation. Continuum radiation is generated by so-called free-free and free-bound interaction of electrons with atoms. Since in both cases the electrons are initially 'free', they can have more or less any energy and therefore we speak of the term continuum.

3.1.1 Brehmstralung

Elastic collisions of charged particles can give rise to a change of momentum, which results in emission of radiation. Since the charged particle is free in both the initial and final state, this radiation is referred to as 'free-free' radiation. In a plasma we can distinguish different interactions between charged particles: electron-electron, electron-ion, electron-atom, ion-atom and ion-ion. The first one is not causing any radiation since no net change in momentum is caused. Any processes involving atoms can be neglected due to the fact that electron-atom contributions are only significant at low degrees of ionization, in the order of 10^{-3}, which is clearly not the case in our plasmas[1]. Besides that, when only heavy particles are involved, their contribution can be neglected, so we will only consider radiation originating from elastic electron-ion collisions. From [7] we know that the emissivity for the 'free-free' radiation of electron-ion collisions is given by:

$$\varepsilon^{\nu}_{ff,ei} = \hat{c}_1 \xi_{ff} \frac{Z_i^{\,2} n_e n_i}{c\sqrt{\hat{T}_e}} \exp(-\frac{h\nu}{e\hat{T}_e}) Wm^{-3}Hz^{-1}sr^{-1}$$

In which c_1=1,5*10^{-45} is an electron-ion constant, ξ_{ff} (equal to 1)is the Biberman factor which contains quantum mechanical corrections for the deviation from a hydrogen plasma, n_e and n_i denote the electron and ion densities respectively, Z_i the atomic number, c the speed of light, T_e the electron temperature in eV, h Planck's constant, ν the frequency and e the electron charge.

This formula can be easily rewritten in terms of the wavelength instead of the frequency. If we now plot this expression over the wavelength regime we're interested in, we find the emissivity due to free-free radiation of the plasma as a function of the wavelength, as depicted in the figure below.

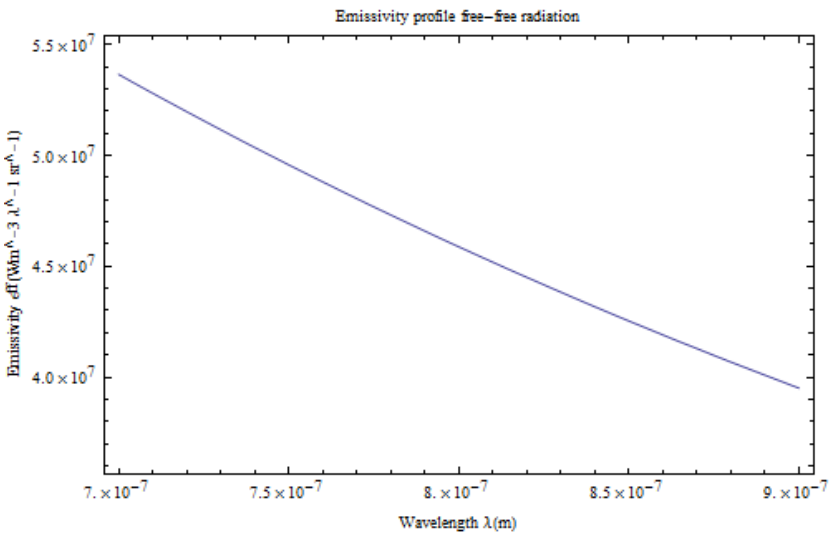

3.1.2 Recombination-radiation

The intensity of the free-bound emission, a free electron gets bound to an ion causing radiation, has the same form as the expression for the Brehmstralung:

$$\varepsilon_{fb}^{\nu} = \frac{\hat{c}_1}{c}\xi_{fb}\frac{n_e^2}{\sqrt{\hat{T}_e}}[1-\exp(-\frac{h\nu}{e\hat{T}_e})]$$

Where ξ_{fb}= ξ_{ff} and c is the speed of light. The emissivity profile of this free-bound radiation decreases faster with increasing wavelength than the free-free emissivity. However, in the 700-900 nm regime, the contribution from the free-bound radiation is about a factor 1,5 higher.

3.1.3 Total continuum radiation

We now treated the different contributions to the continuum emission, so in order to find an expression of the total radiation, involving both free-free and free-bound radiation, one can just easily take the sum of the individual contributions and simplify the result, which yields:

$$\varepsilon_{fb} + \varepsilon_{ff} = \frac{\hat{c}_1}{c}\xi_{tot}\frac{n_e^2}{\sqrt{\hat{T}_e}} \text{ Wm}^{-3}\text{Hz}^{-1}\text{sr}^{-1}$$

where we used the condition of quasi-neutrality of the plasma(n_e=n_i), c_{ei} = c_1 and Z_i = 1 for a hydrogen plasma. In this formula ξ_{tot} represents the total Biberman factor and as this factor corrects for deviation from a hydrogen plasma, we can take it equal to one in our case.

The total emissivity of the plasma can be determined by integrating the sum of the free-bound and free-free emissivities, yielding an emissivity of the plasma, expected in the intended continuum range, of 20,5 $\text{Wm}^{-3}\text{Hz}^{-1}\text{sr}^{-1}$. The total emissivity of the plasma as a function of wavelength is given in the figure below.

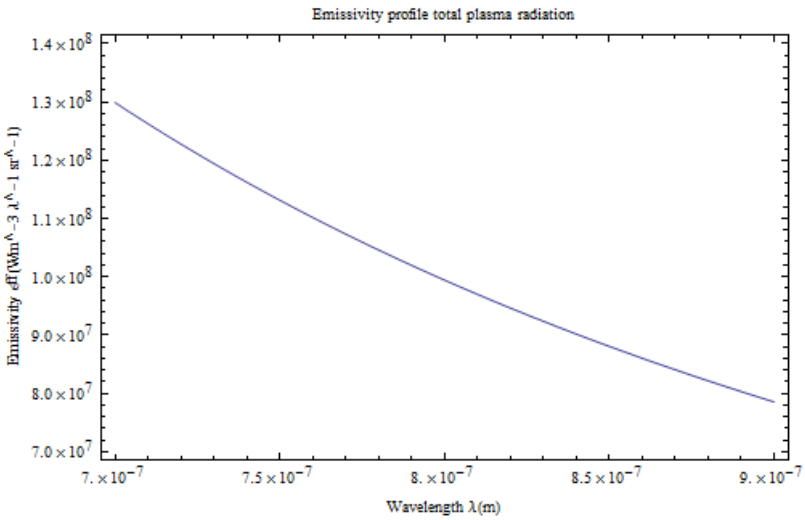

3.2 Abel inversion

When taking lateral spectra of the plasma beam, the camera detects a signal along the line of side, which doesn't give you any relevant physical information about the emissivity of the plasma as a function of the position in the plasma beam.

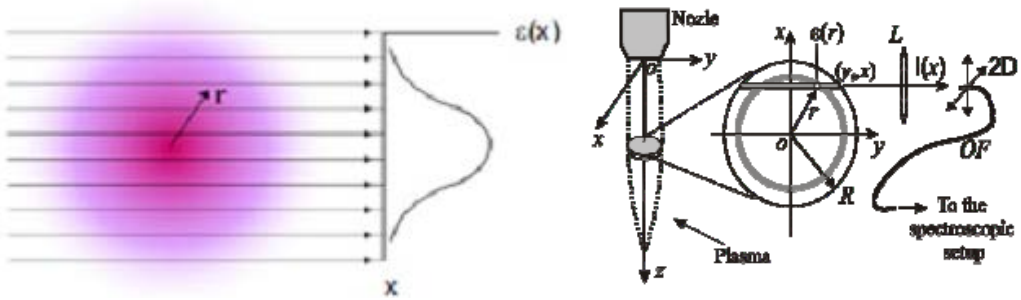

Fig. 7 Left the physical information obtained by integrating over a line of sight. Right a schematic representation of the experimental setup, showing the cross section of the axisymmetric plasma beam and the line-integrating measurement system.

In order to get a radial profile, which does have a physical meaning, out of a line-integrated signal, one has to perform a so-called inverse Abel transform. If the plasma jet is assumed to be cylindrically symmetric and optically thin, then the lateral observed signal can be written as[8]:

$$I(x) = 2\int_{0}^{Y0} \varepsilon(r)dy$$

Where y_0 is the coordinate of the plasma edge for every x value where plasma scanning is performed, as depicted in figure 1. Now, the inverse Abel transform gives us the emissivity ε(r) out of the line-integrated signal I(x)

$$\varepsilon(r) = -\frac{1}{\pi}\int_r^R \frac{I'(x)}{\sqrt{x^2 - r^2}}\,dx$$

4 Continuum measurements

In this section we'll discuss the experiments and their results, from which we obtained the continuum emission profiles. The experimental arrangement that was used for the continuum radiation is described in section 2.4.2, the optical emission spectroscopy set-up. Since the absolute emissivity was measured, the Phantom camera was calibrated by using a well-defined light source. Combined with the quantum efficiency, which was provided in Fig. 6, the sensitivity of the camera was calculated. In conclusion, the validity of the continuum diagnostic was judged.

4.1 Thomson scattering measurements

Alongside our continuum measurements, we performed Thomson scattering, for which the experimental arrangement was provided in section 2.4.1, in order to determine the electron densities and temperatures. In this way we are able to compare our continuum results, which we'd like to use as a diagnostic for the electron density, with the Thomson scattering data to judge the validity of the continuum emission diagnostic.

As Thomson scattering measurements were done over the whole radius of the plasma beam, we are able to construct an electron density profile of the beam as a function of its radius.

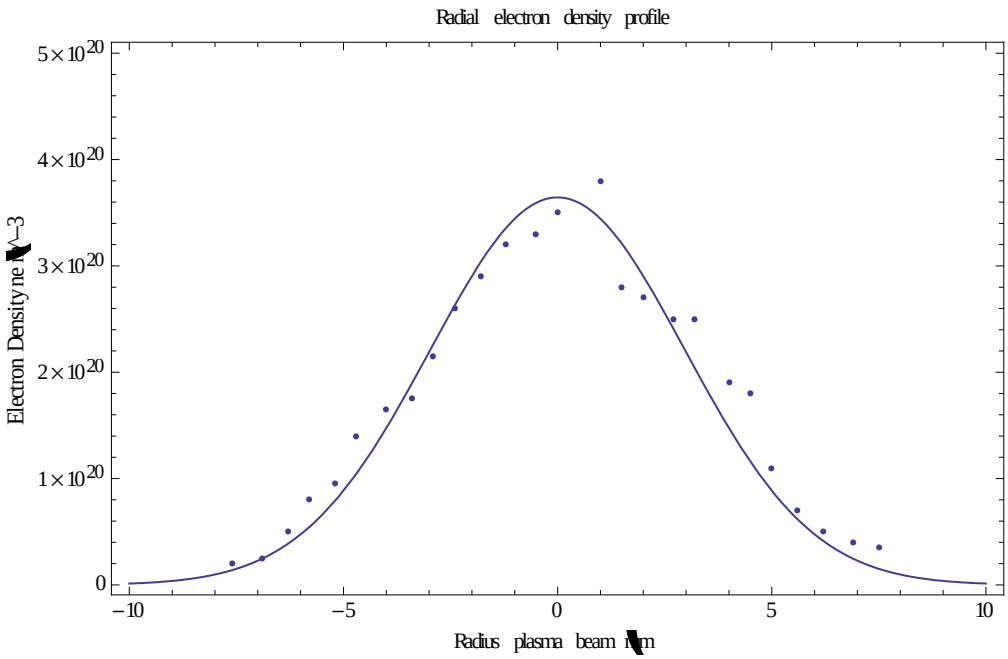

Fig. 8 Fitted electron density(n_e) profile of the plasma beam extracted from Thomson scattering data.

4.2 Results

Now, we need to compare the data obtained from Thomson scattering with the results of our line of sight measurements after applying the inverse Abel transform. Since our line-integrated intensity profiles turned out to be asymmetric, Abel inversion was only performed on one side of the profile, yielding the emissivity profile as depicted in figure 3.

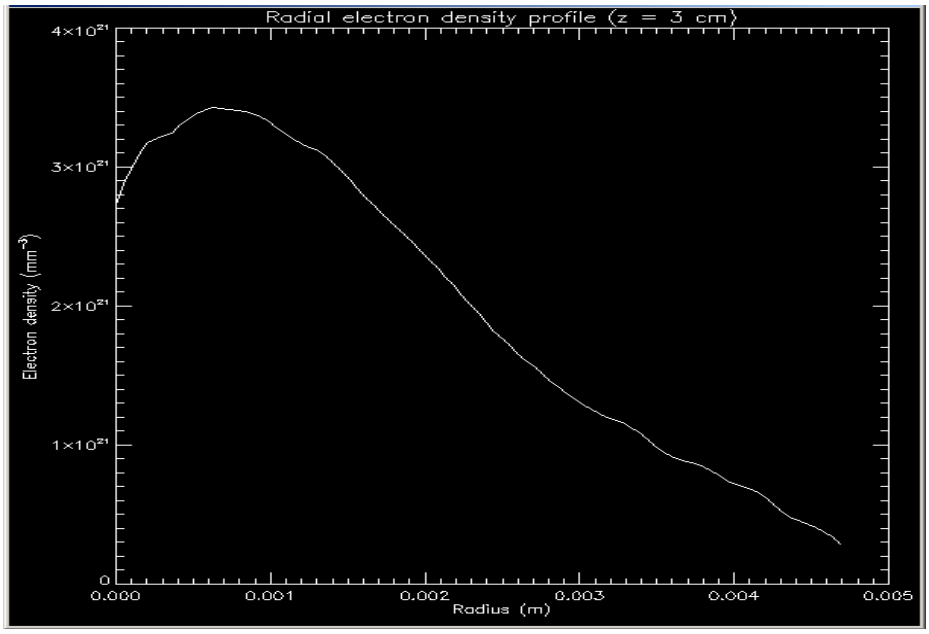

Fig.9 Radial electron density profile obtained by Abel inversion of the line of sight signal. Graph was cut-off at r = 0 due to the asymmetric profile.

These measurements were done for a range of plasma parameters. We've been running the source on 1,5 slm and 2,5 slm hydrogen with a magnetic field of 0.4 T, while having currents of 125 A, 150 A and 175 A. The results of these 6 measurements, producing an electron density profile from both Thomson scattering and Abel inversion of the lateral observed line of sight radiance, are shown below.

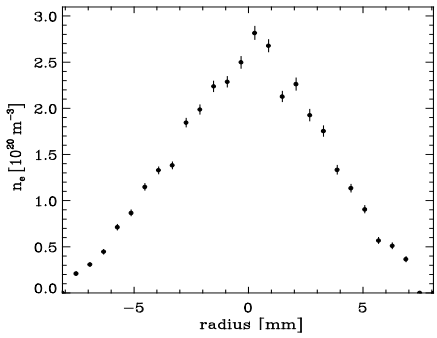

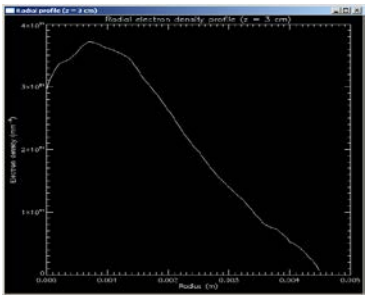

a) 1.5 SLM, 125 A

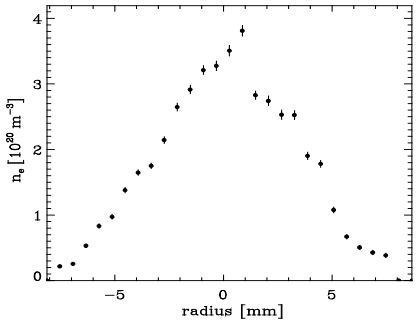

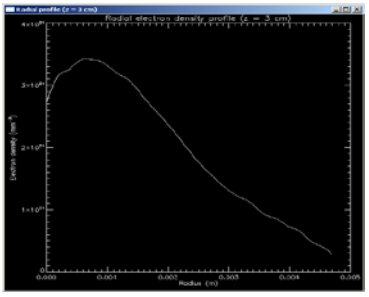

b) 1.5 SLM, 150 A

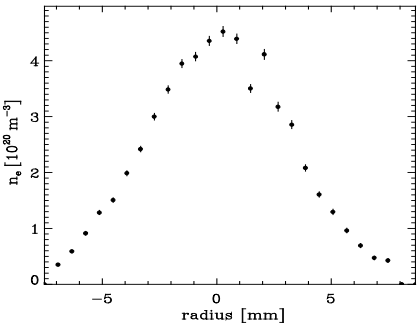

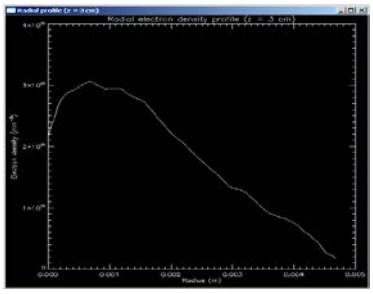

c) 1.5 SLM, 175

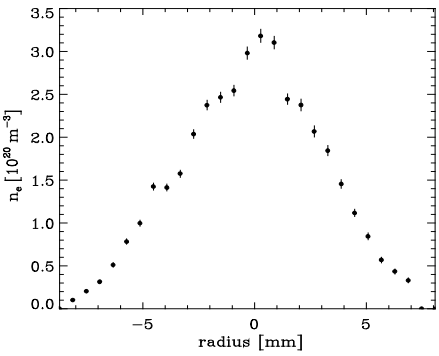

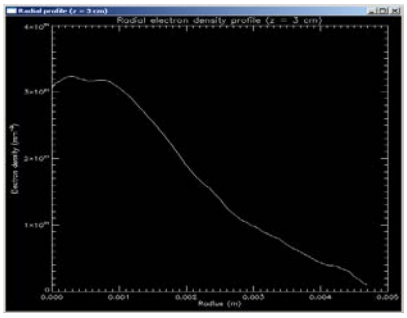

d) 2.5 SLM, 125 A

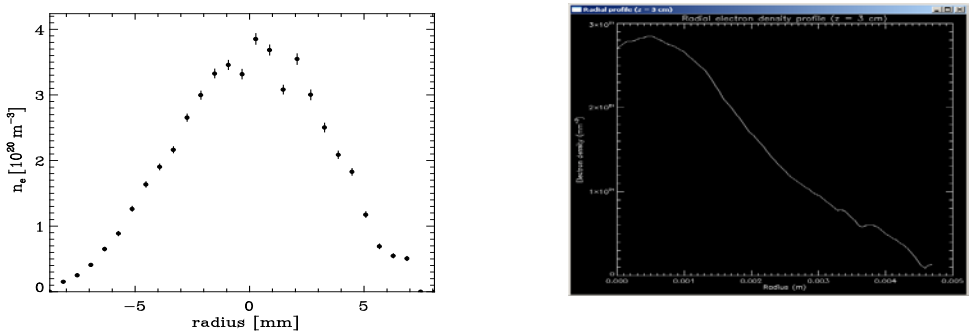

e) 2.5 SLM, 150 A

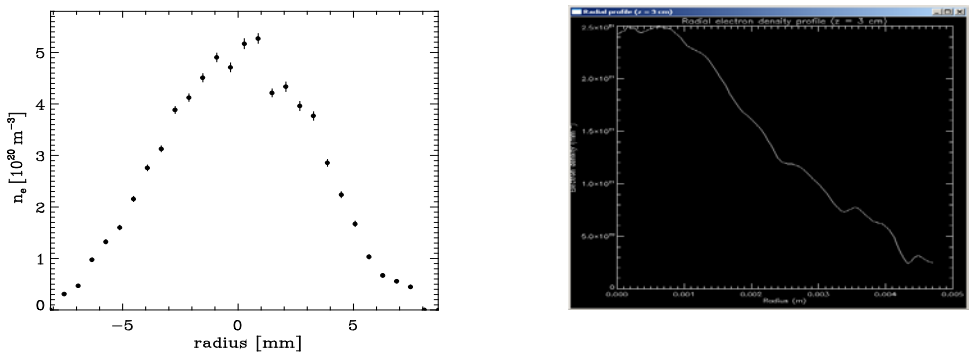

f) 2.5 SLM, 175 A

Fig. In this figure, the results of the Thomson measurements and the continuum measurements, obtained via Abel inversion, are displayed. In both cases, all six radial electron density profiles are provided, i.e. for the source running on 1.5 SLM hydrogen at respectively 125 A(a), 150 A(b) and 175 A(c) and for 2.5 SLM 125 A(d), 150 A(e) and 175 A(f). The white graphs represent the Thomson data, whereas the black graphs are the calculated continuum profiles according to the line of sight integrated signal. The continuum profiles were cut-off at r = 0 because of their asymmetric shape.

4.3 Conclusion and discussion

In order to be able to judge the validity of the continuum emission diagnostic, we compared the absolute electron density profiles from Thomson scattering with those obtained by Abel inversion of the lateral profile. The results show a clear difference between both.

First of all, when comparing the results for the continuum at several currents, we observed something remarkable; the absolute n_e-profile decreases with increasing current, whereas the results from Thomson scattering show a significant increase in absolute density with increasing current, just as we would expect. Secondly, the absolute values of the electron density of the continuum emission profile are roughly an order of magnitude higher than the electron density calculated via the Thomson scattering data in all investigated cases. Moreover, the shape of the continuum emission is concerning. The profiles are quiet asymmetric and besides that they show a hollow emission profile. Our Thomson scattering profiles are asymmetric as well so

that's what we would have expected. Asymmetric profiles could easily be caused by for instance inhomogenety of the axial magnetic field, which influences the confinement of the beam, so that would be a reasonable explanation of the observed asymmetry. However, the hollow emission profiles clearly does not correspond to the Thomson data.

Given the specifications of the Semrock bandpass filter, transmission of line radiation in the near infrared could contribute to our signal and thus raise the detected emission and thereby increase the calculated electron density. Besides that, the possible contribution of emission from a molecular band or from line radiation could cause an overestimation of the electron density. These aspects were investigated as well and their results will be treated in the next chapter.

5 Exploring the discrepancy between Thomson and continuum data

In the previous section we showed our results of the line of sight measurements compared to the obtained Thomson scattering data. We concluded that there's no correlation between both and so we concluded that we've not been looking at real continuum light in the 700-900 nm range. In order to be able to understand this bad correlation, we performed some further experiments on the wavelength range intended for continuum emission measurements.

An Avantes overview spectrometer was installed instead of a CMOS camera in front of the first window of the vessel as depicted in figure 5. The same Semrock-filters and lens were used. The axial position of the focal volume was 3-4 cm in front of the nozzle.

5.1 Emission spectra of 'continuum light'

In these measurements, the same Semrock filters, with central wavelength of 794 nm and width of 160 nm, were used as in the continuum measurements. Experiments were done with and without a magnetic field of 0.4 T. The results with magnetic field, as was the case in our continuum experiments, are shown in figure 10.

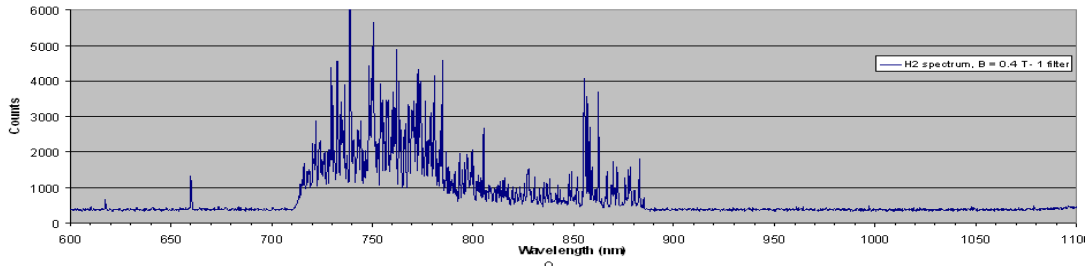

Fig. 10 Measurement of hydrogen plasma at 0.4 T with a Semrock wavelength filter in front of the camera.

The H-α emission at 656 nm is adequately suppressed by the filters, so only significant contribution to the signal comes from roughly the 710-880 nm range. Clearly, there's a lot of line radiation visible in the spectrum, which we don't expect for a hydrogen plasma in this wavelength regime. Besides that, we are even able to distinct a certain emission band between 715-780 nm.

5.2 Analysis of the spectrum

The obtained spectrum in the 715-880 nm range gives rise to discussion, since we are interested in the origin of both the line radiation and the emission band. In this section we'll examine this radiation in order to find a possible explanation for the failing correspondence between our continuum measurements and Thomson data.

Since we don't expect any line-radiation from atomic hydrogen in this wavelength regime, we have been looking for possible contaminations in the plasma. These impurities could be due to contamination of the plasma source(Cu, B, N), contamination of the vessel walls(C) or due to a leakage in the gas feed system(Ar, N). Besides that, there's the possibility to have emission from the hydrogen molecule.

5.2.1 Emission from impurities in the plasma

Let's first have a closer look on the emission lines of the above mentioned possible impurities in our plasma, mainly originating from the source. For the elements copper(Cu), boron(B), carbon(C) and argon(Ar) there seems to be no relevant emission within the very near infrared, the wavelength region we're interested in[9]. However, both the spectrum of nitrogen(N) and molecular hydrogen(H2) deserve special attention.

5.2.2 Nitrogen and NH2 spectra

The spectrum of nitrogen shows some line radiation in our region of interest, namely the 710-800 nm range, which corresponds to our measured spectrum[9], so that could be an indication for the presence of nitrogen in the plasma. If this is the case, we should as well take into account the formation of NH2 molecules, which in turn causes line radiation in the involved wavelength regime.

The emission spectrum of NH2 in the very near infrared(roughly from 700 nm -900 nm, corresponding to 11300 cm^{-1} – 14300 cm^{-1}), was investigated in great detail by *Bachir et al.*[10]. They were able to assign more than 2900 lines in this small region, so there's a rather high probability that these lines contribute to our measured spectrum.

5.2.3 H2 emission in the very near infrared

As we just mentioned, the spectrum of molecular hydrogen should be taken into account when considering our plasma conditions. In general, when concerning discharges in molecular gases, spectra of these type consist not of single, sharp lines but of more or less broad wavelength bands. The measured spectrum in our continuum measurements does show a band structure, roughly ranging from 715 nm to 780 nm, so that's worth having a detailed look on the molecular hydrogen spectrum.

The spectrum of molecular hydrogen has been investigated in the visible optical infrared(VOIR),especially in the 700 nm to 900 nm regime, by *Aguilar et al.*[11], as shown in figure 11. The spectrum was theoretically calculated and compared with the experimental results. Our filters pass wavelengths from approximately 714 nm to 874 nm, so we're interested in that region. Looking at the H2-spectrum, we observe a band from 715 nm to 765 nm, this is in quite good correspondence with the band we observed in our continuum measurements, although that band ranges a bit further to 780 nm.

Besides this band in the H2-spectrum we identify no other bands, only very little lines. Moreover, 'continuum' we can distinguish slowly dies out after approximately 820 nm, which is in fact the case in our measurement as well. Our spectrum shows some lines as well, which could represent the very few lines we observe in the H2-spectrum.

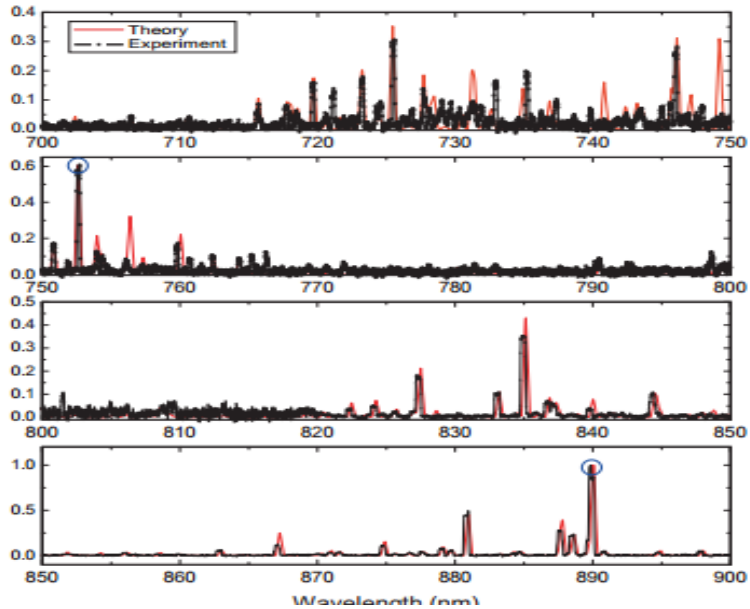

Fig. 11 The spectrum of molecular hydrogen in the near-infrared obtained by [11]. A band structure can be distinguished from 715 nm to 765 nm, which corresponds to the band observed in our continuum experiments.

5.3 Conclusion and discussion

The spectrum of our wavelength regime intended to use for continuum emission is clearly not a smooth continuum spectrum that is to be expected. It reveals a lot of line radiation and even a band structure on top of our continuum. An explanation for these contaminations could be emission from N and NH2, due to residues in the vessel. However, since we assume only little amounts of N(and hence also NH2) in our plasma as it's just a residue, we expect their net contributions to the emission to be rather small.

Besides that, we investigated the emission of the hydrogen molecule. The spectrum of molecular hydrogen shows a rather good correspondence with our measurements. Especially the band ranging from 715-765 nm is comparable with the band structure we observed. Considering the fact that the ionization degree is only up to 15% when exiting the source, the presence of and therefore the emission from molecular hydrogen will be significant. Taking all these things together leaves us the conclusion that it's most likely that emission from molecular hydrogen is responsible for disturbing our continuum spectrum.

6 Origin of emission

In the previous section we used Abel inversion to get a radial emission profile out of a lateral intensity profile, i.e. the emissivity of the plasma as a function of the radial position within the beam is obtained. In this paragraph we'll analyze these radial emission profiles in order to characterize the physical position in the plasma jet from which most emission originates.

6.1 Hollow emission profile

The emission profiles we were able to construct via Thomson scattering are clearly Gaussian shaped, centered at the middle of the plasma beam as shown in figure 12. Since the n_e-profiles from Thomson scattering fit to a Gauss, it's not surprising that the emission profiles show the same radial dependency as the emissivity is proportional to the square of the electron density. Obviously, a Gaussian function centered at r = 0 indicates that the strongest emission comes from the center of the plasma beam.

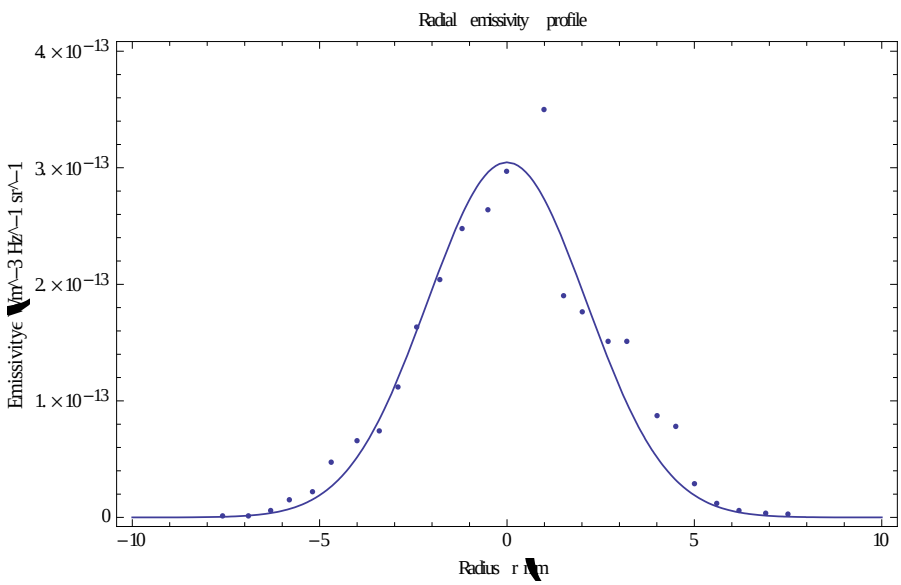

Fig. 12 Radial emission profile centered at r = 0 extracted from the Thomson scattering n_e-profile.

However, as stated before, in the Abel inverted profile we observe a hollow emission profile, indicating most emission originates from a certain distance to the center, whereas the electron density and temperature are substantially less than the maximum value in that region. In fact, considering the whole beam, most light collected seems to be emitted from a ring, where the electron density is lower. This is in accordance with results from *Schumack et al.[5]*, who found

clearly hollow emission profiles by Abel inverting the fit of the intensity profiles, as shown in figure 13.

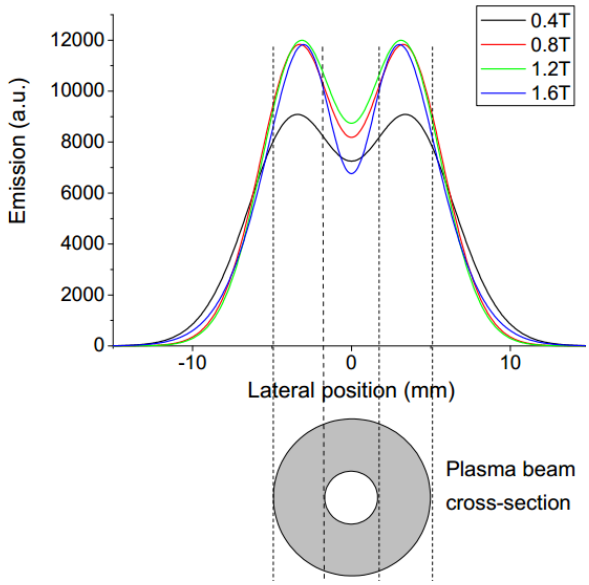

Fig. 13 Radial emission profiles for four magnetic field strengths, obtained by Abel inverting the fit of the intensity profiles. Emission profiles are clearly hollow. A schematic cross-section of the plasma beam is shown indicating positions of strongest emission by shading[5].

6.2 Mechanism causing hollow emission profile

6.2.1 Molecular Activated Recombination and its reaction kinetics

The production of excited neutrals, especially the H*(n=4) atoms, is a crucial factor when considering the emissivity of the hydrogen plasma[5]. These excited neutrals are mostly produced in a sequence of steps via Molecular Activated Recombination(MAR)[12, 13, 14].

H^*(n=4) production

Under Pilot-PSI's plasma conditions, MAR is the main source of the production of excited hydrogen atoms. The first step in this sequence of reactions is the production of a molecular ion by charge exchange between an ion and a rovibrationally excited background gas molecule:

$$H^+ + H_2(r,v) \rightarrow H(1s) + H_2^+(r,v)$$

The produced molecular ion now recombines with an electron and then rapidly dissociates into an excited and a groundstate hydrogen atoms. Due to the energy of the rovibrationally excited molecular ion, the excited state atom will be at least in the n=2 level but most probably in the n=3 level[17]:

$$H_2^+(r,v) + e^- \rightarrow H^* + H(1s)$$

Then, by electron excitation, a H^*(n=4) atom is produced:

$$H^*(n = 2,3) + e^- \rightarrow H^*(n = 4) + e^-$$

In case of quasi-neutrality of the plasma, n_e=n_i, and with n_{H2} of the same order, the rate of MAR is determined by the first step of charge exchanged, which is the slowest.

Reaction kinetics

If we now perform general reaction kinetics on the different steps in the MAR process, we can try to explain the hollow emission profile by seeking for an expression that relates the density of H^*(n=4) to the density of molecular hydrogen. From equilibrium in the first two steps, charge exchange and dissociative recombination, we can write the reaction kinetics as follows:

$$n_{H+} \cdot n_{H2} \cdot k_{cx} = n_{H_2^+} \cdot n_e \cdot k_{dr}$$

$$n_{H_2^+} \cdot n_e \cdot k_{dr} = n_{H(n=3)}(n_e K_3 + A_3)$$

Where k_{cx} and k_{dr} represent the reaction rate of charge exchange and dissociative recombination respectively, K_3 the rate of electron de-excitation from the n=3 level to a lower state, defined as $K_3 \equiv \sum_{i \neq 3} k_{3i}$, and A_3 denotes the rate of spontaneous de-excitation of the H(n=3) level, given by $A_3 \equiv \sum_{i<3} A_{3i}$. Now the balance of H^*(n=4) atoms can be derived from the last step of MAR, the electron excitation :

$$n_{H(n=3)} \cdot n_e \cdot k_{34} = n_{H(n=4)} \cdot (n_e K_4 + A_4)$$

with, analogous to the rate constants mentioned above, $K_4 \equiv \sum_{i \neq 4} k_{4i}$ and $A_4 \equiv \sum_{i<4} A_{4i}$. The terms A_3 and A_4 can be neglected if $n_e > A_4 / K_4$ and $n_e > A_4 / K_4$. If we assume $K_3 \cong k_{34}$, we obtain an expression which relates the excited state population for n=4 to the density of molecular hydrogen:

$$n_{H^+} \cdot n_{H_2} \cdot k_{cx} \cong n_{H(n=4)} \cdot n_e \cdot K_4$$

Hence we find, after assuming quasi-neutrality of the plasma, that:

$$n_{H(n=4)} k_{cx} \cong \frac{n_{H_2} k_{cx}}{K_4}$$

At electron densities above $n_e = 5 \cdot 10^{19}\ m^{-3}$, de-excitation of the H*(n=4) level outweighs radiation[15, 16]. According to the equation above, this process depends only on n_{H2} and not on n_e anymore. As we can extract from our continuum data, this barrier is passed at a plasma radius of roughly 6 mm in our conditions. This means that inside a cylinder with radius of 6 mm, the electron density is above the level at which the emissivity of the plasma is mainly determined by the density of molecular hydrogen. The density profile of n_{H2} is hollow due to the high dissociation degree of the plasma and the short penetration depth of H_2[5]. Since the emission is proportional to both the electron density and molecular hydrogen density for low electron densities and depends only on n_{H2} for higher electron densities, the emission profile will also be hollow, in accordance with the n_{H2}- profile. The result, emission from a ring, is shown in figure 14.

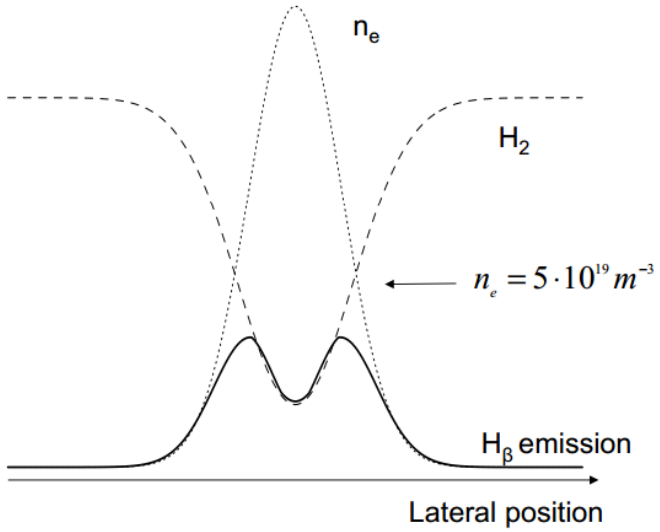

Fig. 14 Expected emission based on the electron density- and molecular hydrogen density-profile. Above $n_e = 5 \cdot 10^{19}\ m^{-3}$ the emission is dominated by the n_{H2}-profile. [5]

6.3 Conclusion and discussion

In our continuum measurements, we observed a hollow radial emission profile of the plasma, which is in contrast with the measured electron densities via Thomson scattering. As the intensity of the continuum radiation should be proportional to the electron density squared, we would have expected the same shaped profile as we observe via Thomson scattering.

However, from MAR and reaction kinetics involved in producing excited state hydrogen atoms, it follows that the emission is dominated by n_{H2} in the core of the plasma beam. This mechanism explains the hollow emission profile we see. Moreover, *Schumack et al.*[5] found radii of about 7-8 mm at which the radiation is expected to be the strongest based on their Thomson scattering measurements. Considering the fact that their experiments were done at a distance of 40 mm from the nozzle, whereas we measured at z = 30 mm, this is in good correspondence with our prediction of 6 mm. As the plasma beam expands when exiting the nozzle, we'd expect a more narrow beam in our experiments. Besides that, their electron densities of the plasma are roughly a factor of 2 lower than ours. These two factors are likely to cause the minor difference between both expectations of the radius of the H_2-dominated parts of the plasma column.

However, the hollow part of our actually observed profile typically covers a radius of around 1-2 mm, instead of the expected 6 mm derived from the reaction kinetics that determine the hollow emission profile. This discrepancy could be caused by overestimating the decay in molecular hydrogen density when entering the center of the plasma in our plasma conditions. When the penetration depth of the H_2 is estimated too short and the dissociation degree of H_2 too high, the H_2-profile will be less hollow. Hence the point at which the density of H_2 decreases significantly will shift towards the center of the plasma beam. So, errors in these two parameters are most likely to cause the differences we see in comparison with theory.

7 Conclusion and discussion

We investigated continuum emission in the near-infrared(700 – 900 nm) from a hydrogen plasma at Pilot-PSI in order to judge its capability as a diagnostic for the electron density and compared this with Thomson scattering experiments, which were done simultaneously. It turns out that there's a threefold discrepancy between them. First of all, the absolute n_e-profile decreases with increasing current, whereas the results from Thomson scattering show a significant increase in absolute density with increasing current. Secondly, the absolute values of the electron density of the continuum emission profile are roughly an order of magnitude higher than the electron density calculated via the Thomson scattering. And lastly, the electron density of the continuum intensity showed a hollow emission profile.

An overview spectrometer was used to examine the spectrum intended for continuum emission and thus the differences in the profiles were explored. Two sources of contamination of the continuum emission were found: a lot of line radiation and even an emission band on top of the 'off-set' of the spectrum. The line radiation could be explained by taking into account emission from impurities in the plasma, mainly N and NH_2, residues in the vessel, whereas the band structure is most likely originating from H_2-molecules, which are pretty abundant in the plasma.

Furthermore, the results were compared with Schumack et al. to explain the hollow emission profile of the continuum emission. Investigation of some underlying plasma processes, which involves Molecular Activated Recombination, leads to the derivation of a model that describes emission dependencies on both n_e and n_{H2}. Above $n_e = 5 \cdot 10^{19}\ m^{-3}$, the emission is dominated by the latter, which implicates a hollow emission profile. However, theoretically we'd expect the hollow part to span a radius of 6 mm, whereas we observed only 1-2 mm. Probably, our plasma conditions don't perfectly suit the model and hence the radius is overestimated.

Taking these things together, the continuum emission in the 700 – 900 nm regime is not suitable for measuring the electron density. At least not in the core of the plasma beam, as the intensity of the emission doesn't depend on the electron density anymore. The 715 – 765 nm regime can't be used either, since the intensity is overcalculated due to the molecular hydrogen emission band.

8 Bibliography

[1] V.P. Veremiyenko, Ph.D. thesis, "An ITER-relevant Magnetized Hydrogen Plasma Jet", Eindhoven University of Technology (2006)

[2] H.J. van der Meiden, Ph.D. thesis, "Thomson scattering on low and high temperature plasmas", Eindhoven University of Technology(2011)

[3] B. de Groot, Z. Ahmad, W.J. Goedheer, N.J. Lopes Cardozo, V. Veremiyenko, Fusion Engineering and Design 66-68, 413-417 (2003)

[4] M.J. de Graaf. Ph.D. thesis University of Technology, Eindhoven, the Netherlands (1994), available on-line at http://alexandria.tue.nl/extra3/proefschrift/PRF10A/9412025.pdf

[5] Amy Shumack et al., "Rotation of a strongly magnetized hydrogen plasma column determined from an asymmetric Balmer-β spectral line with two radiating distributions", Phys. Rev. E 78, 046405 (2008)

[6] Spectral & Color Responses for Phantom Cameras, Vision Research, Inc., Revision 1.0.0 Dated: 07DEC2004

[7] B. van der Sijde, F.J. Hoog, D.C. Schram, "Inleiding plasmafysica", Eindhoven University of Technology(1987)

[8] B. Mitu et al., "Rotational Temperatures in a RF Nitrogen Plasma Jet at Low Pressure", available on-line at http://www.ispc-conference.org/ispcproc/ispc19/407.pdf

[9] NIST Atomic spectra database

[10] H. Bachir et al., "A Combined Analysis of Laser Optogalvanic and Fourier Transform Emission Spectra of NH2 near its Barrier to Linearity", Journal of molecular spectroscopy, 1999 Feb; 193(2): 326-353

[11] Aguilar et al., "Visible to near infrared emission spectra of electron-excited H_2", 2006

[12] N. Ohno, N. Ezumi, S. Takamura, S. I. Krasheninnikov, and A. Yu. Pigarov, "Experimental evidence of molecular activated recombination in detached recombining plasmas," Phys. Rev. Lett., vol. 81, no. 4, 1998.

[13] N. Ezumi, D. Nishijima, and H. Kojima, "Contribution of molecular activated recombination to hydrogen plasma detachment in the divertor plasma simulator NAGDIS-II," J. Nucl. Mater., vol. 337, pp. 266–269, 1999.

[14] M. J. de Graaf, R. Severens, R. P. Dahiya, M. C. M. van de Sanden, and D. C. Schram, "Anomalous fast recombination in hydrogen plasma involving rovibrational excitation," Phys. Rev. E, vol. 48, p. 2098, 1993.

[15] W. L. Wiese, M. W. Smith, and B. M. Glennon, Atomic transition probabilities. Vol.: Hydrogen through Neon. A critical data compilation. National Bureau of Standards, 1966.

[16] J. J. A. M. van der Mullen and D. C. Schram, "On the atomic state distribution function in inductively coupled plasmas-III. Rate coefficients and properties of atomic states," Spectrochim. Acta, Part B: Atomic Spectroscopy, vol. 45B, no. 3, pp. 233–247, 1990.

[17] J. K. Janev, W. D. Langer, J. K. Evans, and J. D. E. Post, Elementary Processes in Hydrogen-Helium Plasmas. Springer-Verlag, 1987.